Cleaner Materials 4 (2022) 100065

Contents lists available at ScienceDirect

Cleaner Materials

journal homepage: www.elsevier.com/locate/clema

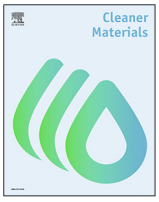

RSM and ANN modelling of the mechanical properties of self-compacting concrete with silica fume and plastic waste as partial constituent replacement

Olatokunbo M. Ofuyatan [a,*], Oghaleoghene B. Agbawhe [a], David O. Omole [a], Chinenye A. Igwegbe [b], Joshua O. Ighalo [b]

[a] Department of Civil Engineering, College of Engineering, Covenant University Ota, Lagos, Nigeria
[b] Department of Chemical Engineering, Nnamdi Azikiwe University, P. M. B. 5025, Awka, Nigeria

ARTICLE INFO

Keywords:
Artificial neural networks
Polyethylene terephthalate
Response surface method
Self-compacting concrete
Silica fume

ABSTRACT

In this study, Response Surface Methodology (RSM) and Artificial Neural Networks (ANN) was used to predict the mechanical properties of self-compacting concrete (SCC) with silica fume as partial cement replacement and Polyethylene terephthalate (PET) solid waste as partial sand replacement. PET plastic was varied between 0 and 20 wt% while the silica fume was varied between 0 and 40 wt%. The parameters investigated were the compressive strength, tensile strength and impact strength of SCC. The RSM model was fairly accurate ($R^2 \geq 0.92$) in predicting the mechanical properties. The model was statistically significant (p-value < 0.5) and did not possess any prediction bias. The ANN model was able to capture the variability of the data as evidenced by the good R^2 threshold ($R^2 > 0.93$) for training, testing and validation. Parity plots revealed that both the ANN and RSM models do not have any prediction bias. However, the ANN model is superior because of its higher accuracy and the use of admixtures enhanced the workability suitability for dataset. The 3D microstructural analysis showed that the interfacial adhesion between the aggregates and the cementitious materials reduced at increased partial replacement leading to a decrease in the strength.

Introduction

Self-compacting concrete (SCC) is a type of concrete that possesses superior flowability and self-compacting ability compared to conventional concrete (Ofuyatan and Edeki, 2018a; Ofuyatan and Edeki, 2018b). It first emerged in Japan in the 1980s (Okamura and Ouchi 2003). Since there is no need for concrete vibrations, its use in construction minimises hearing damages on worksites due to the vibration noises of concrete machines (Meko et al. 2021). It also decreases construction time and ensures enough compaction (Mohammed et al. 2017; Okamura and Ouchi 2003; Ramanathan et al. 2013; Singh and Singh 2018). Partial replacement with solid waste gives SCC a double-pronged advantage. It helps in the reduction of CO2 emissions due to reduced cement use in construction (Meko and Ighalo, 2021a; Meko and Ighalo, 2021b). It also helps in the reduction of solid waste (in cases where they are used as a partial replacement). In this study, Polyethylene terephthalate (PET) is one of the solid wastes used as a partial replacement for sand while silica fume as partial replacement for cement. It is a non-biodegradable solid that pollutes the physical environment and also reduces its aesthetic value (Ahmad et al. 2017; Sulyman et al. 2016).

Over the years, neural network based tools have been employed in the prediction of the properties of concrete (Henigal 2020). As a result, a relationship between the influencing elements, waste plastic and silica fume, and the affected parameters, the compressive, splitting tensile strength and impact test, as output and input variables, will be interesting to develop. To describe the link between the independent and dependent variables, a variety of prediction procedures can be used. RSM and ANN are two techniques of depicting interrelationships that are worth mentioning. RSM is a robust statistical tool highly useful in experimental works to investigate the mathematical association between input and output variables using a small number of trials. It works best in cases where numerous independent variables influence one or more replies.

In the recent review of Ramrakhiani et al. (2019), they observed that Artificial Neural Network (ANN) models are gradually replacing

* Corresponding author.
E-mail address: olatokunbo.ofuyatan@covenantuniversity.edu.ng (O.M. Ofuyatan).

https://doi.org/10.1016/j.clema.2022.100065
Received 31 December 2021; Revised 16 February 2022; Accepted 15 March 2022

conventional linear models for the prediction of concrete properties. ANN models have been used to model systems with fly ash (Azimi-Pour et al. 2020; Douma et al., 2017), silica fume (Awoyera et al. 2020; Rinchon 2017), metakaolin and blast furnace slag (Awoyera et al. 2020) as partial sand replacement. Architectures such as back-propagation neural network (BPNN) (Asteris and Kolovos 2019), genetic programming (GEP) (Awoyera et al. 2020), support vector machine (SVM) (Azimi-Pour et al. 2020), multi-layer perceptron neural network (MLP-ANN) (Sahraoui and Bouziani 2020) and ANN with genetic algorithm (GA-ANN) (Rinchon 2017) have also been explored. Properties modelled in these studies includes creep strain (Al-Rihimy et al. 2019), compressive strength (Meesaraganda et al., 2019; Serraye et al. 2021), tensile strength (Awoyera et al. 2020), flexural strength (Awoyera et al. 2020), chloride concentration resistivity (Rinchon 2017), and fresh properties (Koneru and Ghorpade 2020; Sahraoui and Bouziani 2020). Though SCC with PET have been investigated (Aswatama et al. 2018; Bui et al. 2018; Sojobi et al. 2016), ANN has not been employed to predict SCC mechanical properties from combined silica fume and PET partial sand replacement. Furthermore, the current study also compared the suitability and performance of response surface methodology (RSM) against ANN for the current application. A novel 3D surface reconstruction technique was employed for the microstructural analysis of the experimental samples. In light of these, the novelty of the current study is justified.

The Response Surface Method (RSM) is a collection of mathematical and statistical tools that is useful and effective for modelling and evaluating experimental issues (Rantung et al. 2019). Despite its widespread usage in the design of trials and optimization, this strategy has had limited application in the concrete industry. The response surface was used by Iqbal et al. (2017) to investigate the effects of the SCC mix parameter on several fresh and hardened properties responses, including the slump flow, filling capacity, V-funnel flow time, and compressive strength. Ardalan et al. (2017) employed the RSM to enhance compressive strength while decreasing water sorptivity, water absorption, and chloride permeability in high-performance concrete built with fly ash and metakaolin.

The aim of this study is to utilise Response Surface Methodology (RSM) and Artificial Neural Networks (ANN) to model the mechanical properties of self-compacting concrete (SCC) with silica fume as partial cement replacement and Polyethylene terephthalate (PET) solid waste as partial sand replacement. The study also employed a novel 3D reconstruction technology to investigate the concrete microstructural properties. This is a first study where ANN and RSM performance was compared for SCC with simultaneous partial replacement of concrete and sand using other materials.

Methodology

Experimental

The materials used for the development of the SCC include Portland cement (Dangote brand, grade 42.5 N), granite, river sand, superplasticizer (polycarboxylic ether-based, conplast SP430 to BS-5075 specification), PET, silica fume and water (EN-1008 standard).

Table 2
Sieve analysis of fine and coarse aggregate.

Size of sieve	Sand	PET	Coarse aggregate
12.5 mm	120	120	110
8.5 mm	120	120	45.8
4.75 mm	94.5	91.3	1.0
2.36 mm	85.6	80.6	0.3
1.18 mm	72.1	60.2	–
600 μm	49.9	15.7	–
300 μm	15.2	12.8	–
15 μm	2.8	0.4	–

Table 3
Chemical and physical quality features of Silica fume and Cement.

Components	Cement	Silica fume
CaO	62.86	0.99
SiO_2	20.58	92.54
Al_2O_3	4.90	2.32
Fe_2O_3	4.20	0.57
MgO	2.80	–
SO_3	2.30	0.30
K_2O	0.60	1.01
Na_2O	0.30	0.21
LOI	e	e
Specific Gravity (kg/m^3)	3.09	2.28
Blaine fineness (cm^2/g)	3400	200,000

Table 4
Physical properties of powdered PET.

Physical property of PET	Results obtained
Color	Green
Shape of particle	flat
Thickness	0.22 mm
Specific gravity	1.42
Water absorption (24 h)	–
Tensile strength	59.8 MPa
Bulk density	385.16 kg/m^3
Approx. melting temperature	200–250 °C
Pozzolanic reactivity	135
Fineness	2850

Table 5
Designation of input variables and response.

Designation	Data	Unit	Data band
Factor 1	Plastic	%	$0 \le x \le 20$
Factor 2	Silica fume	%	$0 \le x \le 40$
Factor 3	Time	days	$3 \le x \le 28$
Response 1	Compressive strength	N/mm^2	$10 \le y \le 32$
Response 2	Tensile strength	N/mm^2	$0.8 \le y \le 2.9$
Response 3	Impact strength	kN	$22 \le y \le 135$

Table 1
Design of concrete mix.

	Mix	Cement (kg)	Sand (kg)	Granite (kg)	Silica fume (kg)	Plastic (kg)	Super plasticizer (%)	Water (kg)
1	Control	28	37	42	–	–	2	15
2	PET 5% + SF 10%	25.2	35.15	42	2.8	1.85	2	15
3	PET 10% + SF 20%	22.4	33.30	42	5.6	3.70	2	15
4	PET 15% + SF 30%	19.6	31.45	42	8.4	5.55	2	15
5	PET 20% + SF 40%	16.8	29.60	42	11.2	7.40	2	15

Conplast SP430 is a chloride free, superplasticising admixture based on selected sulphonated napthalene polymers. The PET was melted, cooled and crushed to a fine powder before use. The range of SCC constituents for the mix design in this study was adopted from guidelines in EFNARC (EFNARC, 2002). The design of the concrete mixes is shown in Table 1. The material composition is shown in Table 2, Table 3 and Table 4 for aggregates, cementitious materials and PET respectively. In the concrete, the PET plastic was varied between 0 and 20% by weight, while the silica fume varied between 0 and 40% simultaneously. The compressive strength (ASTM-C39) and tensile strength test of the developed SCC were carried out on compression testing machine (Model YES-2000, England). The impact strength of the SCC was also determined (Model YES-2000, England). All tests were repeated after 3, 7, 21 and 28 days. The results were compiled into a dataset that will be used for the modelling study. The dataset used for the modelling study is available in the Supplementary Material (Table S1). The microstructural analysis was done using SEM (SEM, Phenom proX, Phenom-World BV, The Netherlands) at an acceleration voltage of 15 kV and magnification of × 320 and then analysed by ImageJ v1.53 (Ighalo et al. 2021) for 3D reconstruction.

RSM modelling

RSM is a group of statistical techniques used to investigate and model functional relationships between input variables (x) and response of interest (y) (Khuri and Mukhopadhyay 2010). An RSM polynomial model is given by equation (1) where x is the input variable, y is the output variable, β is a vector of unknown constant coefficients referred to as parameters, ε and is a random experimental error assumed to have a zero mean (Adeniyi et al., 2019). The input variables (known as factors) and the responses are summarised in Table 5.

Table 6
Summary of RSM model accuracy.

Response	Type	R^2	Adjusted R^2	P-value
Compressive strength	Quadratic	0.9664	0.9544	< 0.0001
Tensile strength	Quadratic	0.9228	0.8953	< 0.0001
Impact strength	Quadratic	0.9428	0.9218	< 0.0001

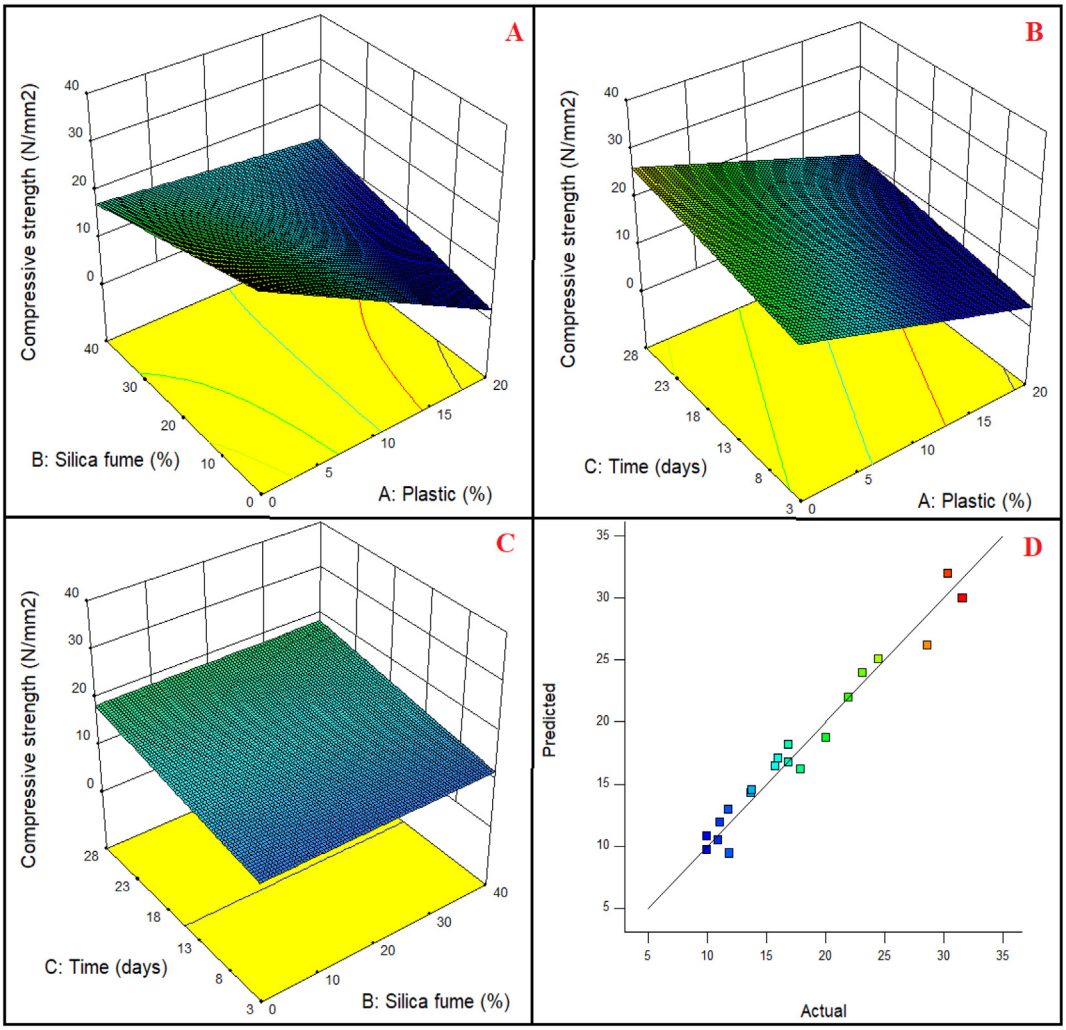

Fig. 1. (a-d). Response surfaces showing the effect of factors on the compressive strength of the SCC (a-c) and the parity plot (d).

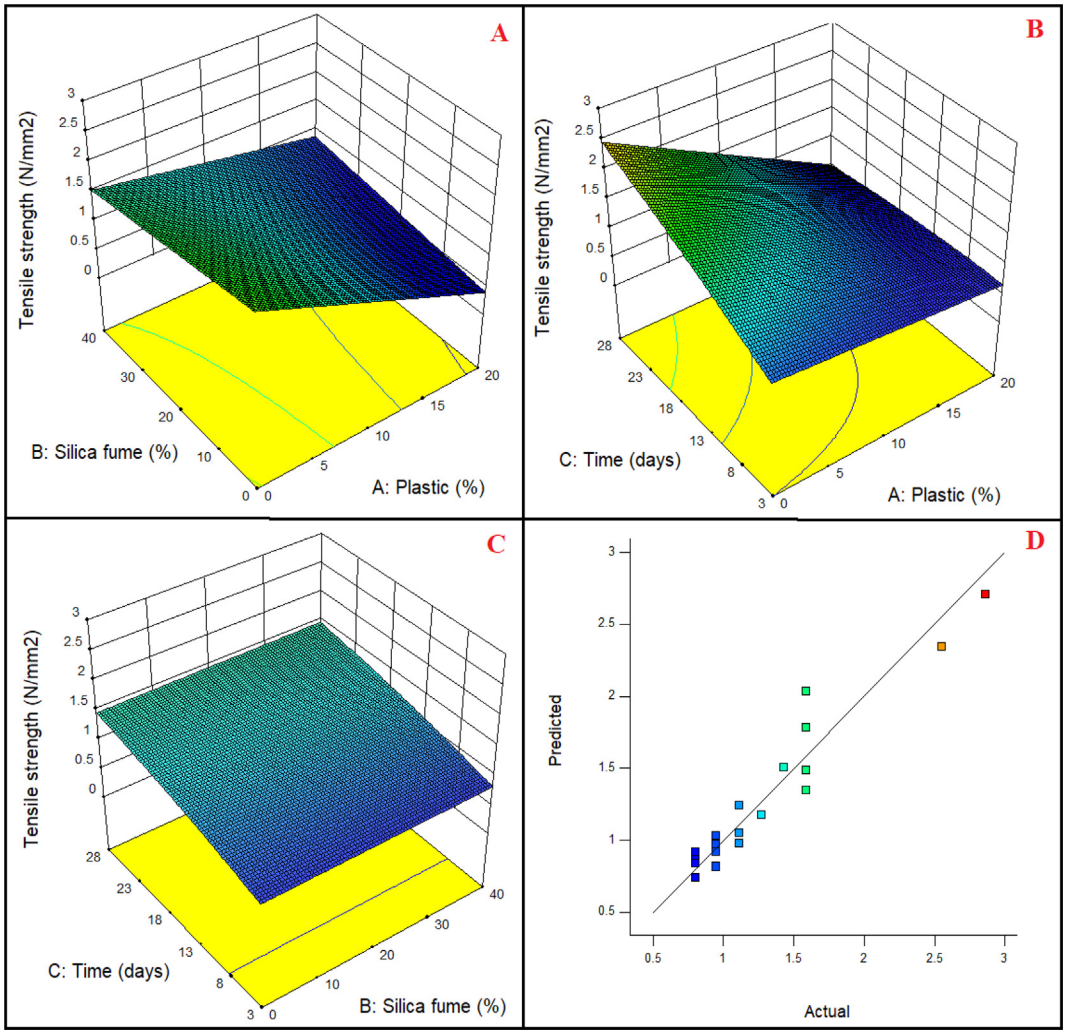

Fig. 2. (a-d). Response surfaces showing the effect of factors on the tensile strength of the SCC (a-c) and the parity plot (d).

RSM modelling was done using historical data design on Design expert v10.0.1 software (Stat Ease Inc., Minneapolis, MN, USA). Historical data design (HDD) is of great advantage because it does not restrict the study to a specific experimental design and it allows the flexibility of inputting any size of data (Ekpotu et al. 2020; Ighalo et al., 2020a).

$$y = \beta_0 + \sum_{i=1}^{k} \beta_i x_i + \sum \sum_{i<j} \beta_{ij} x_i x_j + \sum_{i=1}^{k} \beta_{ii} x_i^2 + \varepsilon \quad (1)$$

ANN modelling

ANN modelling of the mechanical data was done using the Neural fitting tool (nftool) in Matlab 9.4 R2018a (Mathworks Inc., Natick, MA, USA). This was executed using the MLP (multilayer perceptron)-based feed-forward ANN which employs L-M (Levenberge–Marquardt) method to propagation learning algorithm. The basic expression for the neural network is given in equation (2) where Y_j is the output vector, X_i is the input vector, W_1 is the weight vector to hidden layer from inputs, W_2 is the weight vector to output layer from hidden layer, B_1 is the bias vector to hidden layer and B_2 is the bias vector to hidden layer (Pattanayak et al. 2020). The three layers of the ANN network employed include: the input layer (containing %plastic, %silica fume, and curing time), a hidden layer and an output layer (which was either the compressive strength, tensile strength, impact strength). The input layer collects the information given to it and delivers it to the hidden layer for processing, then, the hidden layer performs all the data processing and yields the output (Ghosh et al. 2015). The input data was divided into three categories at random: the training samples of 60%, 20% for validation and 20% for testing. The network was trained by trial-and-error using 1–15 nodes before the proper number of neurons in the hidden layer was obtained after multiple iterations to minimize errors and get the best network topography (Betiku et al. 2015; Ighalo et al. 2020c) which is proved by the decrease in MSE values and the increase in R^2 values for the validation results (Igwegbe et al. 2019). As each neuron is related to all the neurons, these neurons usually communicate by transmitting signals to each other.

$$Y_j = W_2 + \tan sig(W_1 X_i + B_1) + B_2 \quad (2)$$

Results and discussion

RSM modelling

The summarized results of the variance analysis for the 7 days and 28 days compressive, tensile and impact strength of concrete cube specimens of size 150 mm using the response surface model are presented in Table 6. The analysis of variance provides the sum of squares, degree of freedom, mean squares, F value, and p-value at the 5% significance level. It was observed that $R^2 \geq 0.92$ was achieved

for all three responses. The adjusted R^2 is an adjustment/modification of the R^2 that will not become unnecessarily inflated by the addition of variables (it means that only the presence of key variables will contribute to the overall physical interpretation of the response that will increase the adjusted R^2 value). It is better for the adjusted R^2 that is within 0.2 of the R^2. This observation was the case of this study. Furthermore, the p-value reveals that the model is statistically significant at a significance level of $p < 0.5$.

The performance assessment of the inter-relationship between the mix design parameters and the properties of silica fume and plastic reinforced concrete was done and displayed using parity and 3D plots of RSM. The plots for all investigated responses are presented in Fig. 1 (a–c). Fig. 1(a-c) display the parity and 3D plots of dependent variables drawn as function of two independent variables. From the parity and 3D plots of compressive strength shown in Fig. 1(a-c), it was observed that there is no clear interaction between the factor A and B. Reduced strength was observed with reduced B this could be due to reduced water intake as a result of the plastic particles. There was lack of bond between the plastic and the mortar. The effect of the factors is shown in Fig. 1(a-c) for compressive strength, Fig. 2(a-c) for tensile strength and Fig. 3(a-c) for impact strength. It was observed that there was a gradual decrease in the hardened properties of the concrete with increased partial replacement (for both plastic and silica fume). This is consistent with the findings of other SCC studies where materials such as eggshells (Ofuyatan et al. 2020; Yerramala 2014), blast furnace slag (Guo et al. 2020; Ofuyatan et al. 2020), fly ash (Iqbal et al. 2017; Rantung et al. 2019) and pumice (Ardalan et al. 2017) were used as partial cement replacement. Increased curing time also led to improved hardened properties of the concrete as observed from the figures. The work done by Cheng and Sun (2006) revealed a poor bond formation as a result of low strength due to the damage of the surface texture.

From the parity plots in Fig. 1d for compressive strength, Fig. 2d for tensile strength and Fig. 3d for impact strength, it was observed that the predictions lie close to the diagonal this implies that the RSM model could predict the result adequately, with good distribution of the data points above and below the diagonal. This shows that the model does not have over-prediction or under-prediction bias. The major weak-point of the RSM model is that it is aliased meaning that the estimation of the influence of a factor affects the factor itself. The actual and predicted response values clearly shows the closeness of the actual and predicted responses. Significant deviation from normality was not observed in the residual plots; the plots visibly shows that the selected model was suitable in predicting the strength and interaction of the materials used.

ANN modelling

The feasibility of using ANN in the proportioning of SCC mixes was conducted. The result of the ANN modelling is summarised in Table 7. Six different input variables, the percentage of plastic, silica fume used; the curing time; and strength data for the compressive, tensile

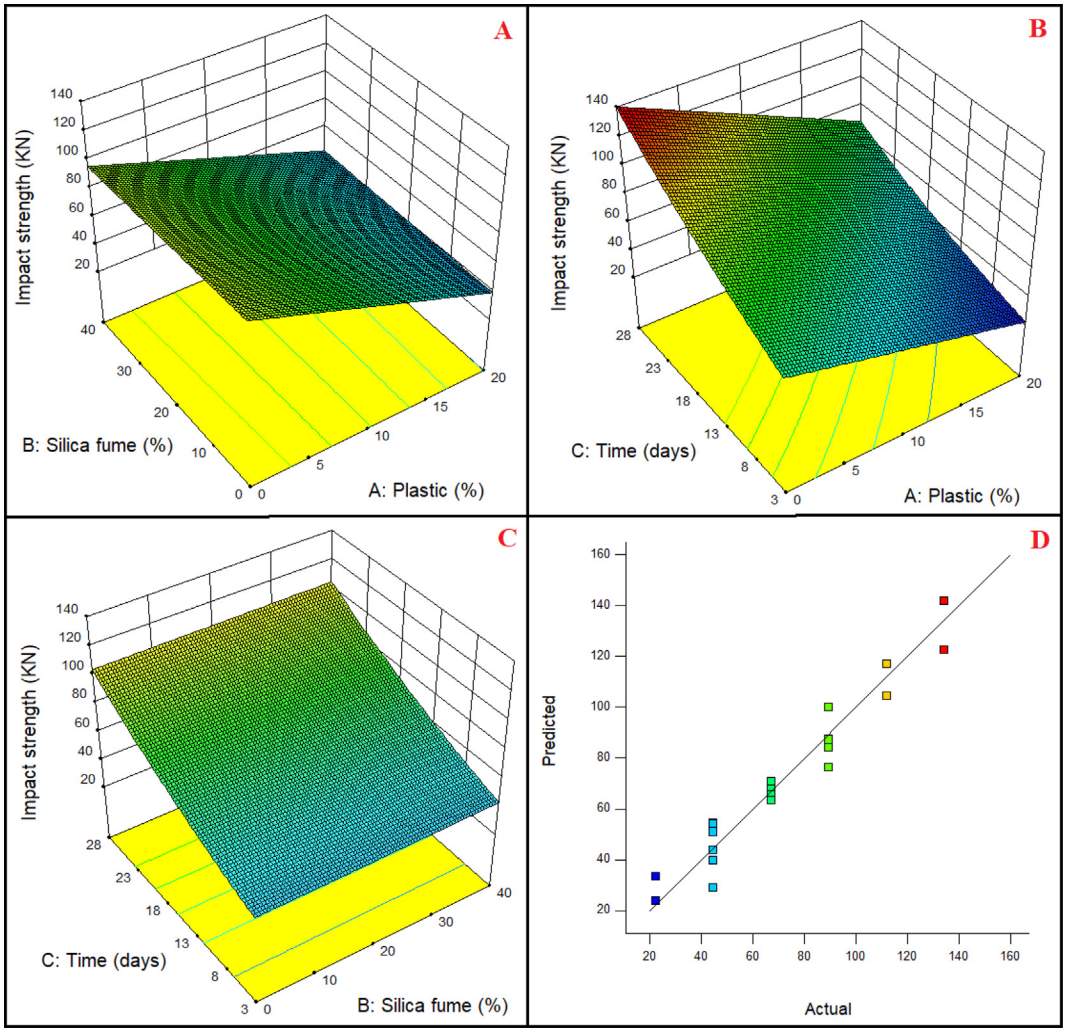

Fig. 3. (a-d). Response surfaces showing the effect of factors on the impact strength of the SCC (a-c) and the parity plot (d).

Table 7
Summary ANN modelling results for the study.

Response	Phase	Model accuracy	
		MSE	R^2
Compressive strength	Training	0.0483	0.9989
	Validation	1.0917	0.9945
	Testing	3.2371	0.9636
Tensile strength	Training	0.0069	0.9925
	Validation	0.0223	0.9318
	Testing	0.0009	0.9784
Impact strength	Training	8.5539	0.9953
	Validation	82.429	0.9715
	Testing	68.251	0.9983

and impact were selected as the input variables for ANN modelling. The 28 day strength of the concrete was the only output variable.

Table 7 presents the Mean Squared Error (MSE) of ANN model during the training process based on input data. The least MSE in the validation step happened at epoch 16 which has the best validation performance equal to 82.4291. It is worth mentioning that model training keeps going as long as the error of the network on the validation vector is reducing. In addition, the analysis stop point is equal to 22, i.e. 6 error repetitions after the epoch with the best validation performance, i.e. epoch 16. The models were assessed by the mean squared error (MSE) and the coefficient of determination (R^2). The models captured the variability of the data as evidenced by the good R^2 threshold ($R^2 > 0.93$) for training, testing and validation. However, the MSE of the impact strength was considerably poor compared to that of the other two responses. The parity plots for compressive strength, tensile strength and impact strength are shown in Fig. 4(a-c) respectively. Based on the even distribution of points around the diagonals, it can be summarised that the model does not have a bias to always over-predict or under-predict the results. The validation performance of the ANN model at each epoch for compressive strength and tensile strength is given in the Figure S1-S3 respectively.

Microstructural analysis of the concrete surface

The 3D microstructure of the concrete surface with increasing partial replacement of cement is shown in Fig. 5(a-e) at a magnification of × 500. From the images, the valleys (usually in purple) represents regions of poor interfacial adhesion between the aggregates in the concrete and the cementitious materials (Ofuyatan et al. 2021). These characteristic valleys can be observed to increase with each micrograph of increased partial replacement. This suggests that the hardened properties of the concrete reduce due to a reduction in this interfacial adhesion. Though the interfacial transition zone (ITZ) might not be directly apparent from a microstructural image, the surface implications (the outlines of the deep valleys) are a direct implication of its presence. In summary, the 3D microstructural analysis reveals that the interfacial adhesion between the aggregates and the cementitious materials reduced at increased partial replacement leading to poorer hardened properties. When the concrete constituents have good interfacial adhesion, an incidental effect on the concrete surface would not lead to significant deformation. However, poor interfacial adhesion would result to the dislodging of some adhered particles by an incidental force thereby compromising the surface integrity of the concrete.

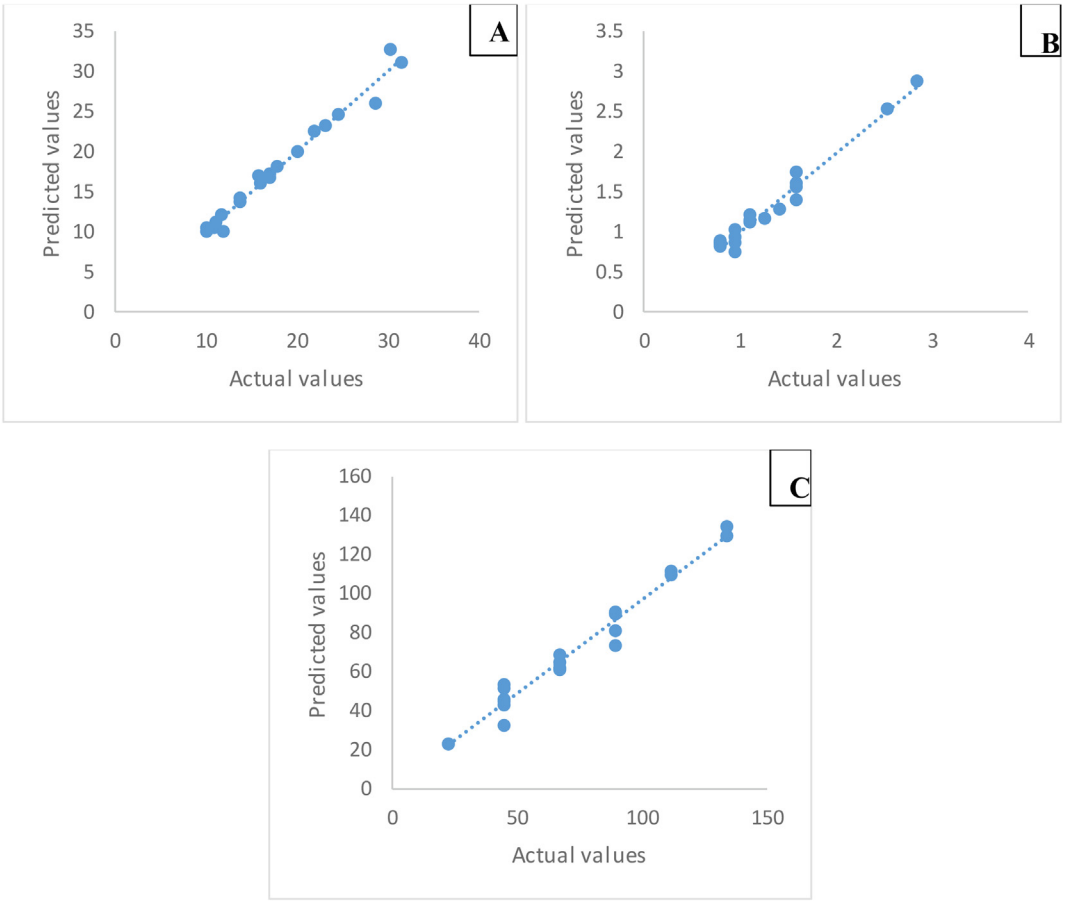

Fig. 4. (a-c). Parity plots for the ANN modelling for compressive strength (a), tensile strength (b) and impact strength (c).

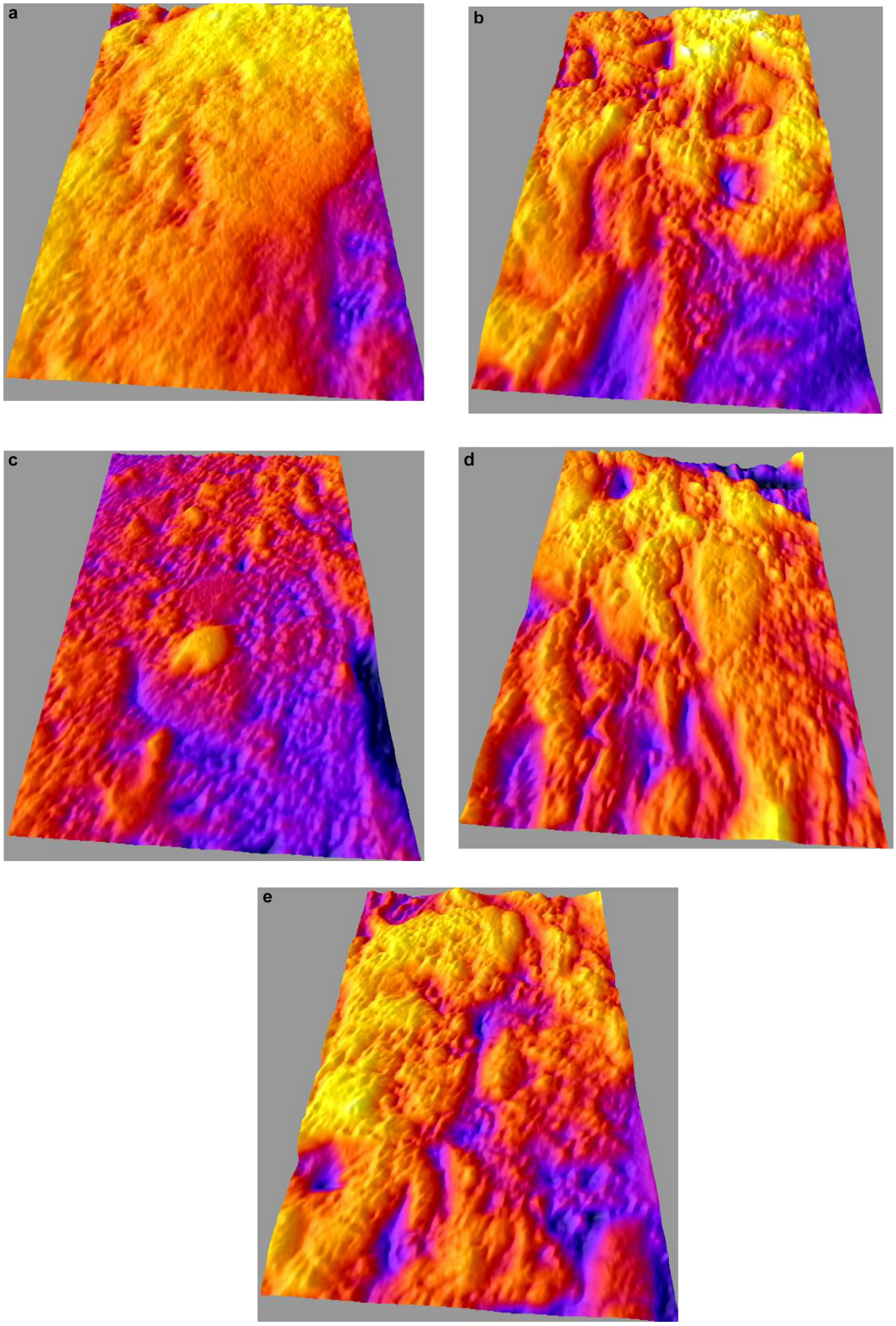

Fig. 5. a. 3D microstructure of the control specimen at 28 days (magnification of × 500) B. 3D microstructure of the specimen containing PET 5% + SF 10% at 28 days (magnification of × 500) 5c. 3D microstructure of the specimen containing PET 10% + SF 20% at 28 days (magnification of × 500) d. 3D microstructure of the specimen containing PET 15% + SF 30% at 28 days (magnification of × 500) e. 3D microstructure of the specimen containing PET 20% + SF 40% at 28 days (magnification of × 500).

Practical implications of the study

The findings of this study have several practical relevance to civil and environmental engineers. Design models such as these are important in preliminary design estimations of product performance (Adeniyi et al. 2021) based on a target replacement of cement with other solid wastes. Given the environmental advantages of reduced cement use, the choice of the extent of partial replacement must be carefully considered and the need to maintain the regulatory minimum threshold of mechanical performance of the concrete. In cases like this, predictive models are relevant and useful. Furthermore, prediction models such as this are also relevant in the budgetary considerations, financial feasibility analysis and preliminary costing of civil engineering project. ANN predictions are fast and less expensive compared to theoretical and/or experimental techniques (Ighalo et al., 2020b).

The current study utilised a novel 3D reconstruction technology based on the SEM analysis. This represents a new paradigm in research in self-compacting concrete where 3D visualisation of the concrete microstructure is possible (Schmid et al. 2010) as opposed to the direct vertical view of the conventional SEM analysis. From an environmental standpoint, the study bears positive implications for the environment. Reduced cement usage leads to lesser CO2 emissions (Ighalo and Adeniyi 2020). Using solid wastes as partial replacement is a viable waste management technique (Hossain et al. 2017).

Conclusion

In this study, RSM and ANN were used to model the hardened properties of SCC with silica fume and PET solid waste as partial constituent replacement. Some important conclusions were derived from the study.

(1) The workability assessed on the fresh properties showed that the 10% PET + 20% SF attained the same slump as the control mix which satisfied ERFNAC recommendation.
(2) A decrease in strength was observed as the percentage replacement of the admixture increased.
(3) From the microstructural studies, with minimal replacements, C – S – H gels were formed, and the rate of hydration was similar to the reference concrete, as seen with mix 2. However, with more significant substitutions, the C – S – H gels were reduced as well as the chemical reaction between particles. The presence of voids was visible in mix 5, which had the effect of weakening the concrete.
(4) The use of ANN and RSM models, have shown to be helpful and efficient models for predicting compressive strength based on experimental results.
(5) Using the ANN and RSM approaches, we have obtained more information with fewer trial mixes.
(6) The RSM model was fairly accurate ($R^2 \geq 0.92$) in predicting the hardened properties of the concrete. The model was statistically significant ($p < 0.5$) and did not possess any prediction bias. Its main weakness was that it was aliased.
(7) The ANN model was able to capture the variability of the data as evidenced by the good accuracy ($R^2 > 0.93$) at the training, testing and validation stages.
(8) Parity plots revealed that both the ANN and RSM models do not have any prediction bias. However, the ANN model is superior because of its higher accuracy and suitability for the dataset.
(9) The 3D microstructural analysis reveals that the interfacial adhesion between the aggregates and the cementitious materials reduced at increased partial replacement leading to poor hardened properties. The model is relevant for project design and budgetary predictions.

Disclosure statements

Compliance with Ethical Standards: This article does not contain any studies involving human or animal subjects.

Declaration of Competing Interest

The authors declare that they have no known competing financial interests or personal relationships that could have appeared to influence the work reported in this paper.

Appendix A. Supplementary data

Supplementary data to this article can be found online at https://doi.org/10.1016/j.clema.2022.100065.

References

Adeniyi, A.G., Ighalo, J.O., Odetoye, T.E., 2019. Response surface modelling and optimisation of biodiesel production from Avocado plant (Persea americana) oil. Indian Chem. Eng. 62 (3), 243–250.

Adeniyi, A.G., Igwegbe, C.A., Ighalo, J.O., 2021. ANN Modelling of the Adsorption of Herbicides and Pesticides based on Sorbate-Sorbent Interphase. Chem. Africa 4 (2), 443–449.

Ahmad, A.F., Razali, A.R., Razelan, I.S.M., 2017. Utilization of polyethylene terephthalate (PET) in asphalt pavement: A review. IOP Conf. Ser.: Mater. Sci. Eng. 203, 012004.

Al-Rihimy, A., Al-Shathr, B., Al-Attar, T., 2019. Prediction of Creep Strain for Self-Compacting Concrete by Artificial Neural Networks Kufa. J. Eng. 10 (2), 90–100.

Ardalan RB, Joshaghani A, Hooton RD (2017) Workability retention and compressive strength of self-compacting concrete incorporating pumice powder and silica fume Construction and Building Materials 134:116-122.

Asteris, P.G., Kolovos, K.G., 2019. Self-compacting concrete strength prediction using surrogate models. Neural Comput. Appl. 31 (S1), 409–424.

W, K.A., Suyoso, H., U, N.M., Tedy, P., 2018. The Effect of Adding PET (Polyethylen Terephthalate) Plastic Waste on SCC (Self-Compacting Concrete) to Fresh Concrete Behavior and Mechanical Characteristics. J. Phys.: Conf. Ser. 953, 012023.

Awoyera, P.O., Kirgiz, M.S., Viloria, A., Ovallos-Gazabon, D., 2020. Estimating strength properties of geopolymer self-compacting concrete using machine learning techniques. J, Mater. Res. Technol. 9 (4), 9016–9028.

Azimi-Pour, M., Eskandari-Naddaf, H., Pakzad, A., 2020. Linear and non-linear SVM prediction for fresh properties and compressive strength of high volume fly ash self-compacting concrete. Constr. Building Materials 230, 117021.

Betiku, E., Okunsolawo, S.S., Ajala, S.O., Odedele, O.S., 2015. Performance evaluation of artificial neural network coupled with generic algorithm and response surface methodology in modeling and optimization of biodiesel production process parameters from shea tree (Vitellaria paradoxa) nut butter. Renewable Energy 76, 408–417.

Bui, N.K., Satomi, T., Takahashi, H., 2018. Recycling woven plastic sack waste and PET bottle waste as fiber in recycled aggregate concrete: An experimental study. Waste Manage (Oxford) 78, 79–93.

Cheng, E., Sun, X., 2006. Effects of wood-surface roughness, adhesive viscosity and processing pressure on adhesion strength of protein adhesive. J. Adhes. Sci. Technol. 20 (9), 997–1017.

Belalia Douma, O., Boukhatem, B., Ghrici, M., Tagnit-Hamou, A., 2017. Prediction of properties of self-compacting concrete containing fly ash using artificial neural network. Neural Comput. Appl. 28 (S1), 707–718.

EFNARC S (2002) Guidelines for self-compacting concrete London, UK: Association House 32:34.

Ekpotu, W.F., Ighalo, J.O., Nkundu, K.B., Adeniyi, A.G., 2020. Analysis of Factor Effects and Interactions in A Conventional Drilling Operation by Response Surface Methodology and Historical Data Design. Petroleum Coal 62, 1356–1368.

Ghosh, A., Das, P., Sinha, K., 2015. Modeling of biosorption of Cu (II) by alkali-modified spent tea leaves using response surface methodology (RSM) and artificial neural network (ANN). Appl. Water Science 5 (2), 191–199.

Guo, Z., Jiang, T., Zhang, J., Kong, X., Chen, C., Lehman, D.E., 2020. Mechanical and durability properties of sustainable self-compacting concrete with recycled concrete aggregate and fly ash. Constr. Build. Mater. 231, 117115.

Henigal, A., 2020. Design of Self Compacting Concrete Using Artificial Neural Networks (Dept. C) MEJ Mansoura. Eng. J. 37 (2), 50–73.

Hossain, M.U., Poon, C.S., Lo, I.M., Cheng, J.C., 2017. Comparative LCA on using waste materials in the cement industry: A Hong Kong case study Resources. Conserv. Recycl. 120, 199–208.

Ighalo, J.O., Adelodun, A.A., Adeniyi, A.G., Igwegbe, C.A., 2020. Modelling the Effect of Sorbate-Sorbent Interphase on the Adsorption of Pesticides and Herbicides by Historical Data Design Iranica Journal of. Energy Environ. 11, 253–259.

Ighalo, J.O., Adeniyi, A.G., 2020. A perspective on environmental sustainability in the cement industry. Waste Disposal Sustainable Energy 2 (3), 161–164.

Ighalo, J.O., Adeniyi, A.G., Igwegbe, C.A., 2021. 3D Reconstruction and Morphological Analysis of Electrostimulated Hyperthermophile Biofilms of Thermotoga neapolitana. Biotechnol. Lett. 43 (7), 1303–1309.

Ighalo, J.O., Adeniyi, A.G., Marques, G., 2020. Application of Artificial Neural Networks in Predicting Biomass Higher Heating Value: An Early Appraisal. Energy Sources Part A: Recovery, Utilization, Environmental Effects, 1–9.

Ighalo JO, Igwegbe CA, Adeniyi AG, Abdulkareem SA (2020c) Artificial Neural Network Modeling of the Water Absorption Behavior of Plantain Peel and Bamboo Fibers Reinforced Polystyrene Composites Journal of Macromolecular Science, Part B:1-13.

Igwegbe, C.A., Mohmmadi, L., Ahmadi, S., Rahdar, A., Khadkhodaiy, D., Dehghani, R., Rahdar, S., 2019. Modeling of adsorption of Methylene blue dye on Ho-CaWO4 nanoparticles using Response surface methodology (RSM) and Artificial neural network (ANN) techniques. MethodsX 6, 1779–1797.

Iqbal, S., Ali, A., Holschemacher, K., Ribakov, Y., Bier, T.A., 2017. Effect of fly ash on properties of self-compacting high strength lightweight concrete. Periodica Polytechnica Civ. Eng. 61, 81–87.

Khuri, A.I., Mukhopadhyay, S., 2010. Response surface methodology. Wiley Interdiscip. Rev. Comput. Stat. 2 (2), 128–149.

Koneru, V.S., Ghorpade, V.G., 2020. Assessment of strength characteristics for experimental based workable self compacting concrete using artificial neural network. Materials Today: Proceedings 26, 1238–1244.

Meesaraganda LP, Saha P, Tarafder N (2019) Artificial Neural Network for Strength Prediction of Fibers' Self-compacting Concrete. In: Soft Computing for Problem Solving. Springer, pp 15-24.

Meko, B., Ighalo, J.O., 2021. Utilization of Cordia Africana wood sawdust ash as partial cement replacement in C 25 concrete. Cleaner Materials 1, 100012.

Meko, B., Ighalo, J., Jiao, P., 2021. Utilization of waste paper ash as supplementary cementitious material in C-25 concrete: Evaluation of fresh and hardened properties. Cogent Eng. 8 (1).

Meko, B., Ighalo, J.O., Ofuyatan, M.O., 2021. Enhancement of Self-Compactability of Fresh Self-Compating Concrete: A Review. Cleaner Materials 1, 100019.

Mohammed, B.S., Achara, B.E., Nuruddin, M.F., Yaw, M., Zulkefli, M.Z., 2017. Properties of nano-silica-modified self-compacting engineered cementitious composites. J. Cleaner Production 162, 1225–1238.

Ofuyatan, M.O., Adeniyi, A.G., Ighalo, J.O., 2021. Evaluation of fresh and hardened properties of blended silica fume self-compacting concrete (SCC). Research Eng. Struct. Mater. 7, 211–223.

Ofuyatan, M.O., Adeniyi, A.G., Ijie, D., Ighalo, J.O., Oluwafemi, J., 2020. Development of High-Performance Self Compacting Concrete Using Eggshell Powder and Blast Furnace Slag as Partial Cement Replacement. Constr. Build. Mater. 256, 119403.

Ofuyatan, O.M., Edeki, S.O., 2018. Dataset on predictive compressive strength model for self-compacting concrete. Data Brief 17, 801–806.

Ofuyatan, O.M., Edeki, S.O., 2018. Dataset on the durability behavior of palm oil fuel ash self compacting concrete. Data Brief 19, 853–858.

Okamura, H., Ouchi, M., 2003. Self-Compacting Concrete. J. Adv. Concrete Technol. 1 (1), 5–15.

Pattanayak, S., Loha, C., Hauchhum, L., Sailo, L., 2020. Application of MLP-ANN models for estimating the higher heating value of bamboo biomass. Biomass Conversion Biorefinery, 1–10.

Ramanathan, P., Baskar, I., Muthupriya, P., Venkatasubramani, R., 2013. Performance of self-compacting concrete containing different mineral admixtures KSCE journal of. Civ. Eng. 17, 465–472.

Ramrakhiani, L., Ghosh, S., Mandal, A.K., Majumdar, S., 2019. Utilization of multi-metal laden spent biosorbent for removal of glyphosate herbicide from aqueous solution and its mechanism elucidation. Chem. Eng. J. 361, 1063–1077.

Rantung, D., Supit, S.W.M., Nicolaas, S., 2019. Effects of different size of fly ash as cement replacement on self-compacting concrete properties. J. Sustainable Eng.: Proc. Series 1 (2), 180–186.

Rinchon, J.P.M., 2017. Strength durability-based design mix of self-compacting concrete with cementitious blend using hybrid neural network-genetic algorithm IPTEK. J. Proc. Series 3.

Sahraoui, M., Bouziani, T., 2020. ANN modelling approach for predicting SCC properties-Research considering Algerian experience. Part I. J. Build. Mater. Struct. 7, 188–198.

Schmid, B., Schindelin, J., Cardona, A., Longair, M., Heisenberg, M., 2010. A high-level 3D visualization API for Java and ImageJ. BMC Bioinf. 11, 1–7.

Serraye, M., Kenai, S., Boukhatem, B., 2021. Prediction of Compressive Strength of Self-Compacting Concrete (SCC) with Silica Fume Using Neural Networks Models. Civil Eng. J. 7, 118–139.

Singh, N., Singh, S., 2018. Evaluating the performance of self compacting concretes made with recycled coarse and fine aggregates using non destructive testing techniques. Constr. Build. Mater. 181, 73–84.

Sojobi, A.O., Nwobodo, S.E., Aladegboye, O.J., Pratico, F.G., 2016. Recycling of polyethylene terephthalate (PET) plastic bottle wastes in bituminous asphaltic concrete. Cogent Eng. 3 (1), 1133480.

Sulyman, M., Haponiuk, J., Formela, K., 2016. Utilization of recycled polyethylene terephthalate (PET) in engineering materials: a review International. J. Environ. Sci. Devel. 7, 100.

Yerramala, A., 2014. Properties of concrete with eggshell powder as cement replacement. Indian Concr. J. 88, 94–105.